IEEE Photonics Journal
An IEEE Photonics Society Publication

Open Access

Adaptive Postdistortion for Nonlinear LEDs in Visible Light Communications

Volume 6, Number 4, August 2014

H. Qian, Senior Member, IEEE
S. J. Yao
S. Z. Cai
T. Zhou

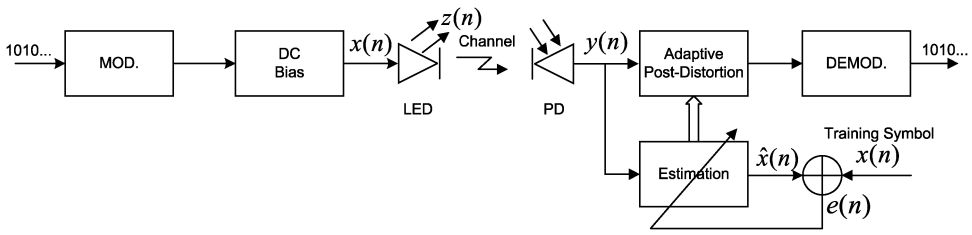

DOI: 10.1109/JPHOT.2014.2331242
1943-0655

IEEE photonics SOCIETY

IEEE

Adaptive Postdistortion for Nonlinear LEDs in Visible Light Communications

H. Qian, *Senior Member*, *IEEE*, S. J. Yao, S. Z. Cai, and T. Zhou

Shanghai Institute of Microsystem and Information Technology, Chinese Academy of Sciences, Shanghai 200050, China
Key Laboratory of Wireless Sensor Network and Communications, Chinese Academy of Sciences, Shanghai 200050, China
Shanghai Research Center for Wireless Communications, Shanghai 200050, China

DOI: 10.1109/JPHOT.2014.2331242

Manuscript received April 4, 2014; revised May 28, 2014; accepted June 3, 2014. Date of publication June 17, 2014; date of current version June 26, 2014. This work was supported in part by the National Natural Science Foundation of China under Grant 61231009 and in part by the Shanghai Science and Technology Development Project under Grants 11DZ1500201 and 12511503400. Corresponding author: H. Qian (e-mail: hua.qian@shrcwc.org).

Abstract: In a visible light communication (VLC) system, the light-emitting diode (LED) is the major source of nonlinearity. The nonlinear effects in the VLC system are different from the conventional wireless communications system. The channel separation in the VLC system is significantly larger than the signal bandwidth; thus, the adjacent channel interference is not an issue. Predistortion technique may not be a cost-efficient approach since it needs additional feedback physical circuits at the transmitter. In this paper, we propose a postdistortion technique to estimate and compensate for the LED's nonlinearity at the receiver. The postdistortion technique only needs some additional computational resources. In addition, the proposed approach significantly improves the error-vector-magnitude and bit-error-rate performance of the VLC system. Simulation results validate the theoretical analysis.

Index Terms: VLC, nonlinearity, memory effects, Wiener model, post-distortion, memory polynomial model.

1. Introduction

The wireless spectrum of the conventional radio frequency (RF) system is very limited and is not able to meet the increasing demand for mobile data traffic. VLC is an attractive alternative as it has many advantages, such as almost unlimited bandwidth, license-free operation, chip front-end, etc. [1]. To achieve a high data rate transmission, orthogonal frequency-division multiplexing (OFDM) technique has been widely used in VLC systems [2]. The OFDM signals are modified to other specific OFDM signal formats, such as DC biased optical OFDM (DCO-OFDM) and asymmetrically clipped optical OFDM (ACO-OFDM), to accommodate the fact that the LED in the transmitter only works with real and positive input [3]. Such signals are sensitive to the LED's nonlinearity in the VLC system due to their high peak-to-average power ratio (PAPR).

In [4] and [5], the nonlinear behavior of the LED was discussed in detail. The nonlinear characteristics of the LED's V–I curve are shown in the blue line in Fig. 1. The LED has a turn on voltage (TOV). If the input voltage is smaller than TOV, the LED is considered as cut-off and is not conducting current. Therefore, a DC bias is applied to guarantee that the input signal works

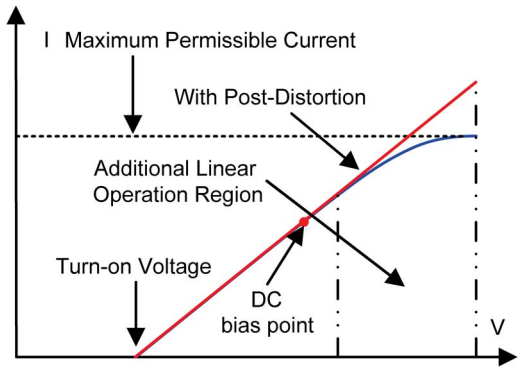

Fig. 1. Nonlinear and linearized transfer characteristics of the LED. Post-Distortion helps to linear the *V–I* curve of the LED.

in the LED's operation region. However, the LED's response exhibits nonlinearity for large input signals [6]–[8]. Increasing the magnitude of the signal will drive the LED into the nonlinear region, thus exhibits nonlinear effects [9], [10]. In addition, the LED has a maximum permissible current, which limit the maximum magnitude of the input signal. Moreover, the carrier-density response is indeed frequency depended, thus introducing memory effects to the LED [11].

Previous works, such as [12] and [13], presented predistortion methods to mitigate the nonlinearity of the LED. In [12], the authors designed predistortion circuits, which only consists of diodes and resisters, to compensate for the nonlinearity. In [13], the authors measured the forward voltage and forward current of the LED and estimated the inverse characteristic of the LED's *V–I* curve with memoryless polynomial model by using these electronic measurements. A *V–V* block with inverse nonlinear behavior of the LED was inserted before the LED to compensate for its nonlinearity. However, these predistortion methods may not be cost-efficient approaches as they need additional physical circuits at the transmitter. In addition, the memory effects of the LED's nonlinearity were neglected in [13]. In [14], the authors applied the Volterra equalization for the compensation of the LED's nonlinearity with memory effects. However, solving the Volterra coefficients needs a lot of computational resources, especially for high order Volterra kernels. In addition, the data rate decreases as the Volterra equalizer converges with a great deal of training sequences [14].

In this paper, we propose an adaptive post-distortion technique to mitigate the LED's nonlinearity with memory effects at the receiver. On one hand, unlike the wireless communications system, the channel separation in the VLC system is significantly larger than the signal bandwidth, thus the ACI performance is not an issue. On the other hand, the adaptive post-distortion only needs some computational resources without any additional physical circuits at the receiver. The adaptive post-distortion technique is more cost-efficient than the adaptive predistortion technique and is easier for implementation compared to the Volterra equalizer. The red line in Fig. 1 shows the linearized *V–I* curve with the post-distortion technique.

The rest of paper is organized as follows. Section 2 introduces the VLC system with adaptive post-distortion technique. The Wiener model is applied to describe the LED's nonlinearity with memory effects and the memory polynomial model is utilized to track and compensate for the nonlinearity with memory effects. Section 3 validates the effectiveness of adaptive post-distortion technique with an AWGN channel in terms of EVM, BER, and constellation diagram performance. Section 4 concludes this paper.

2. System Architecture and the Post-Distortion Technique

As the LED only works with real and positive input voltages, the conventional OFDM signal are modified to other formats, such as ACO-OFDM and DCO-OFDM [15]. Fig. 2 shows the block diagrams of a DCO-OFDM VLC system with adaptive post-distortion technique. In the transmitter

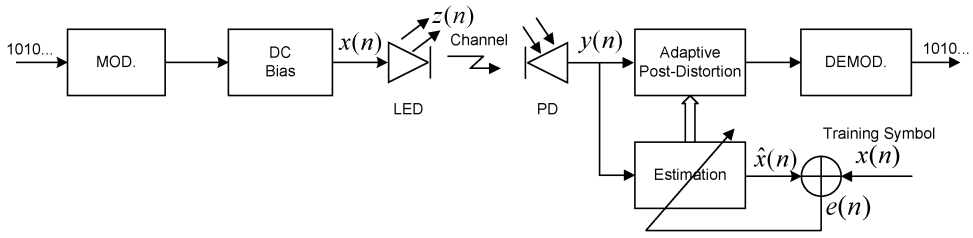

Fig. 2. Block diagrams of a DCO-OFDM VLC system with adaptive post-distortion technique.

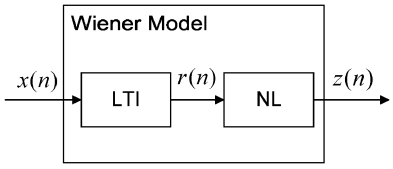

Fig. 3. The Wiener model consists of a linear time-invariant (LTI) block and a memoryless nonlinear (NL) block.

path, the information bits are modulated and assigned to all positive subcarriers and the data on negative subcarriers are complex conjugate of the data on positive subcarriers. By adding a high DC bias, the bipolar signal is converted to unipolar signal before modulating the LED intensity. Training signal $x(n)$ is the input of the LED whereas $z(n)$ is the output of the LED. The output voltage of the PD is $y(n)$, which is considered as linear with the light intensity. The training signal $x(n)$ and its corresponding receive signal $y(n)$ are used to estimate the inverse characteristics of the LED. A copy of the estimation block is inserted between the PD output and the traditional receiver path to compensate for the LED's nonlinearity with memory effects.

The LED exhibits nonlinear effects as the number of emitted photons is not proportional to the injected current amplitude. Moreover, the carrier-density response is indeed frequency depended, thus giving rise to memory effects of the LED [11]. In [11], it is verified that the Volterra series models achieved better accuracy than the static approaches to describe the commercial LED's nonlinearity with memory effects.

The nonlinearity with memory effects can be described by Volterra model, memory polynomial model, Wiener model, Hammerstein model, etc. In this paper, we assume that the LED's nonlinearity with memory effects follows an Wiener model, which consists of a linear time-invariant (LTI) block and a memoryless nonlinear (NL) block [16]. Fig. 3 shows the block diagrams of the Wiener model. The LTI block can be presented as

$$r(n) = \sum_{l=0}^{L-1} b_l x(n-l), \tag{1}$$

where L is the maximum delay tap. The NL block can be described with a Rapps model, which is commonly used to describe the nonlinearity of the power amplifier (PA) in radio frequency (RF) systems. In order to model the V–I curve of the LED, the Rapps model with some simple modifications is given by [17], [18]

$$z(n) = \begin{cases} \dfrac{(r(n)-V_{TOV})}{\left(1+\left(\frac{r(n)-V_{TOV}}{I_{\max}}\right)^{2k}\right)^{\frac{1}{2k}}}, & r(n) \geq V_{TOV} \\ 0, & r(n) < V_{TOV}. \end{cases} \tag{2}$$

In (2), $I_{\max}$ is the maximum permissible current of the LED and k is the knee factor, which controls the smoothness of the transition from the linear to the saturation region.

In theory, the Hammerstein model is the exact inverse of the Wiener model [19]. For an arbitrary LED, however, it may not completely obeys the Wiener model. In order to guarantee the robustness of the adaptive post-distortion technique, we apply memory polynomial model [20], which is a general form of Hammerstein model, to describe the inverse nonlinear characteristics of the LED

$$\hat{x}(n) = \sum_{k=1}^{K} \sum_{d=0}^{D} \alpha_{k,d} y^k (n-d) \tag{3}$$

where K is the number of polynomial terms, D is the maximum delay tap, and $\alpha_{k,d}$ is the model coefficient.

Let us define the new vector notations as follows:

$$\boldsymbol{\alpha} = [\alpha_{1,0}, \alpha_{2,0}, \ldots, \alpha_{K,0}, \ldots, \alpha_{1,D}, \alpha_{2,D}, \ldots, \alpha_{K,D}]^T \tag{4}$$

$$\boldsymbol{y}(n) = \left[y(n), y^2(n), \ldots, y^K(n), \ldots, y(n-D), y^2(n-D), \ldots, y^K(n-D)\right], \tag{5}$$

where $(\cdot)^T$ denotes the matrix transpose. Therefore, (3) can be rewritten as

$$\hat{x}(n) = \boldsymbol{y}(n)\boldsymbol{\alpha}. \tag{6}$$

The error signal can be given by

$$e(n) = x(n) - \hat{x}(n) = x(n) - \boldsymbol{y}(n)\boldsymbol{\alpha}. \tag{7}$$

By minimizing the power of the error signal, the LS solution can be obtained. The objective function can be presented as

$$\text{argmin}_{\alpha} \sum_{n=0}^{N-1} |e(n)|^2 = \text{argmin}_{\alpha} \sum_{n=0}^{N-1} |(x(n) - \boldsymbol{y}(n)\boldsymbol{\alpha}|^2. \tag{8}$$

The LS solution to (8) is given by

$$\boldsymbol{\alpha} = (\boldsymbol{Y}^H \boldsymbol{Y})^{-1} \boldsymbol{Y}^H \boldsymbol{x} \tag{9}$$

where

$$\boldsymbol{x} = [x(0), x(1), \ldots, x(N-1)]^T \tag{10}$$

$$\boldsymbol{Y} = \begin{bmatrix} \boldsymbol{y}(0) \\ \boldsymbol{y}(1) \\ \vdots \\ \boldsymbol{y}(N-1) \end{bmatrix} \tag{11}$$

and $(\cdot)^H$ denotes the Hermitian transpose.

As indicated in (9), the matrix inversion during model coefficients estimation may come at some expense of delay. Therefore, we derived the recursive least squares (RLS) solution of (8) as follows [21]:

$$\boldsymbol{P}(n) = \left(\boldsymbol{I} - \frac{\boldsymbol{P}(n-1)\boldsymbol{y}^H(n)\boldsymbol{y}(n)}{1 + \boldsymbol{y}(n)\boldsymbol{P}(n-1)\boldsymbol{y}^H(n)}\right)\boldsymbol{P}(n-1) \tag{12}$$

$$\boldsymbol{\alpha}(n) = \boldsymbol{\alpha}(n-1) + \frac{\boldsymbol{P}(n-1)\boldsymbol{y}^H(n)}{1 + \boldsymbol{y}(n)\boldsymbol{P}(n-1)\boldsymbol{y}^H(n)}(z(n) - \boldsymbol{y}(n)\boldsymbol{\alpha}(n-1)) \tag{13}$$

where $\boldsymbol{P}(n)$ is the inversion of $\boldsymbol{Y}^H\boldsymbol{Y}$, obtained from the first n samples. $\boldsymbol{P}(n)$ is initialized by $\boldsymbol{P}(-1) = \lambda^{-1}\boldsymbol{I}$, where λ is an arbitrary small constant. In the context of post-distorter coefficients

TABLE 1

Details of the Wiener LED model

LTI			NL		
b_0	b_1	b_2	I_{max}	k	V_{TOV}
1	0.15	0.1	0.5	2	0.2

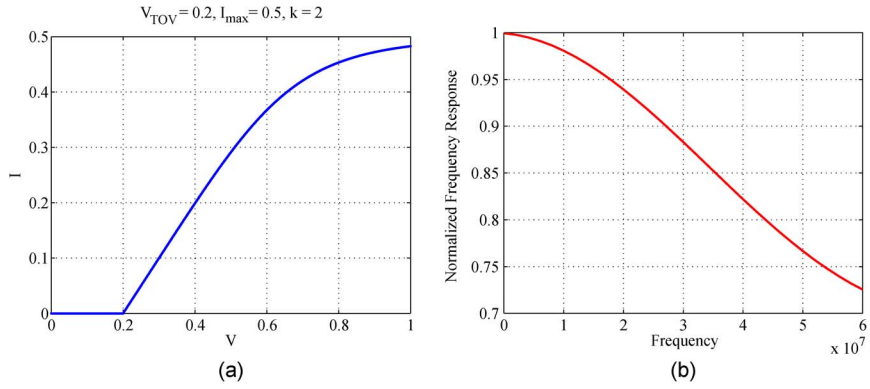

Fig. 4. (a) Transfer characteristics of the Rapps model. (b) Frequency response of the Wiener LED model.

TABLE 2

Harmonic distortion values with and without post-distortion

Values	Basis	Third-order	Fifth-order
Without PD	0dB	-14.86dB	-27dB
With PD	0dB	-49.77dB	-50.44dB

estimation, it is natural to set $\alpha(-1) = [1, 0, \ldots, 0]^T$. As indicated in (12) and (13), the computational complexity of RLS algorithm is on the order of $\boldsymbol{O}((K \times (D+1))^2)$.

3. Simulation

In this simulation, the LED's nonlinearity with memory effects is described by a Wiener model, whose parameters are shown in Table 1. For the LTI block, b_0, b_1, and b_2 are the weighting factors of each delay tap. For the NL block, the maximum permissible current $I_{\text{max}} = 0.5$, the knee factor $k = 2$, and the TOV $V_{TOV} = 0.2$. Fig. 4(a) shows the transfer characteristics of the NL block and Fig. 4(b) shows the frequency response of the Wiener LED model. The frequency response of the Wiener LED model is not flat, which indicates that the LED exhibits memory effects.

Nonlinear effects are normally measured in harmonic distortion. In this paper, we first apply a 1 MHz single tone signal with 40 dB SNR to the nonlinear LED. As shown in Table II, the third-order and fifth-order harmonic distortions are significant. With post-distortion, the reductions to the harmonic distortions are 34.91 dB and 23.44 dB, respectively. The result shows that the post-distortion is effective in the presence of nonlinearity.

In order to further verify the effectiveness of our proposed adaptive post-distortion technique, we test its performance in a modulated DCO-OFDM VLC system. In this paper, we focus on the signals with OFDM formats, however, the post-distortion still works with other modulation formats as well. The DCO-OFDM setup details are listed in Table 3. The IFFT length is 128, where the positive sub-carriers are assigned with data and the negative sub-carriers are assigned with

TABLE 3

Setup details of the DCO-OFDM system

Bias point	IFFT length	DATA sub-carriers	Training Symbols	Mapping	Symbol Rate	Data Rate
0.6	128	63	8	64QAM	100K sym/s	37.8Mbps

the complex conjugate of the data. Each sub-carrier is modulated with uncoded 64-quadrature amplitude modulation (QAM) constellations (6 bits per symbol). The symbol rate is 100 K sym/s and the data rate is 37.8 Mbps. For the purpose of real-time implementation, RLS algorithm is utilized to estimate the model coefficients with 8 training symbols. In order to compensate for the LED's nonlinearity adaptively, we estimate the model coefficients at the beginning of each packet. In a packet duration, we assume that the LED's nonlinearity is constant.

The VLC channel can be modeled as a line-of-sight (LOS) channel and the multi-path effects are negligible [1]. In other words, the inter symbol interference (ISI) is negligible in the VLC systems. Therefore, we apply an additive white Gaussian noise (AWGN) channel in this simulation. For uncoded 64 QAM modulation, the approximate signal to noise ratio (SNR) value required to achieve a target BER of 10^{-5} is 20 dB. The PD is considered as a linear device. We apply memory polynomial model to track and compensate for the LED's nonlinearity with memory effects. Various polynomial terms and various power back-offs are tested in this simulation to achieve the target BER.

3.1. BER and EVM

In the first study, simulations are conducted to verify the effectiveness of our proposed adaptive post-distortion technique in terms of BER and EVM performance enhancement. The EVM is calculated by

$$EVM = 10\log\frac{1}{N_{sym}}\frac{1}{N_{sc}}\frac{1}{P_0}\sum_{i=1}^{N_{sym}}\sum_{j=1}^{N_{sc}}\Big((I(i,j)-I_0(i,j))^2+(Q(i,j)-Q_0(i,j))^2\Big), \tag{14}$$

where N_{sym} denotes the number of symbols, N_{sc} denotes the number of data sub-carriers, $(I(i,j), Q(i,j))$ and $(I_0(i,j), Q_0(i,j))$ denote the observed and ideal symbol point at the ith OFDM symbol, jth sub-carrier of the OFDM symbol in the complex plan, respectively, and P_0 is the average power of the constellation.

In this simulation, the BER and EVM is computed over 1000 OFDM symbols with 63 data sub-carriers. In Fig. 5, from top to bottom, the red line shows the BER/EVM without post-distortion, the blue line shows the BER/EVM with post-distortion $(\mathrm{K}=2,\mathrm{D}=2)$, the green line shows the BER/EVM with post-distortion $(\mathrm{K}=4,\mathrm{D}=2)$, the black line shows the BER/EVM with post-distortion $(\mathrm{K}=6,\mathrm{D}=2)$, and the pink line shows the BER/EVM with post-distortion $(\mathrm{K}=8,\mathrm{D}=2)$.

In Fig. 5, we observe that the adaptive post-distortion with memory polynomial model achieves satisfactory performance in terms of BER and EVM. The BER and EVM performance increases with the polynomial terms and/or the power back-offs. In addition, the black line and the pink line are almost converging, which indicates that the polynomial terms $K=6$ is good enough to compensate for the LED's nonlinearity.

In Fig. 5(a), the BER values without post-distortion are saturated at 4×10^{-3} with the increasing of the power back-off. At 0 dB power back-off, in other words, the modulation index is 2/3, the BER values with post-distortion are higher than 10^{-5} for all cases. With the increasing of the power back-off, all the BER curves with memory polynomial model are saturated at 1.2×10^{-5}. More specifically, the memory polynomial model $((K=6,D=2)$ needs 2 dB power back-off whereas the memory polynomial model $(K=4,D=2)$ needs 5 dB. In Fig. 5(b), the EVM curves are with same trends as that of Fig. 5(a).

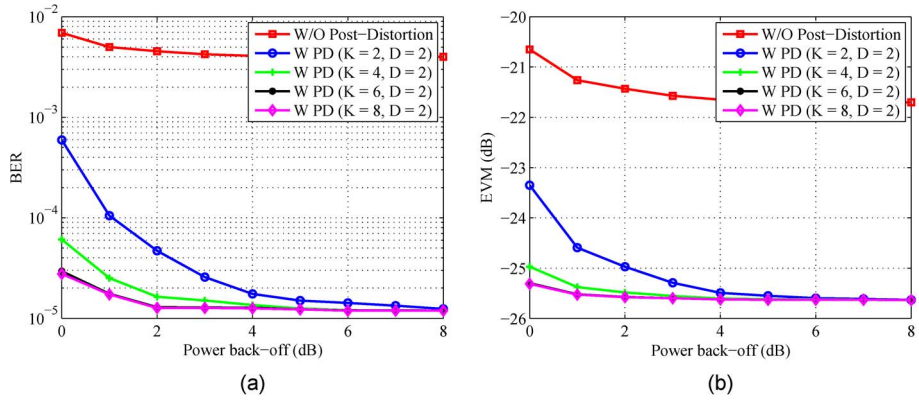

Fig. 5. (a) BER curves, (b) EVM curves. From top to bottom, the red line shows the BER/EVM without post-distortion, the blue line shows the BER/EVM with post-distortion $(K = 2, D = 2)$, the green line shows the BER/EVM with post-distortion $(K = 4, D = 2)$, the black line shows the BER/EVM with post-distortion $(K = 6, D = 2)$, and the pink line shows the BER/EVM with post-distortion $(K = 8, D = 2)$.

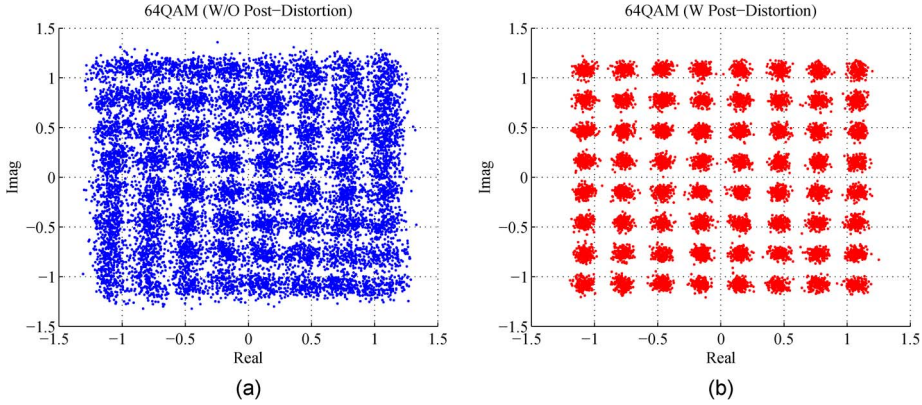

Fig. 6. Constellation diagrams with 20 dB SNR and 1 dB power back-off. (a) Shows the Constellation diagram of 64 QAM modulation without post-distortion. (b) Constellation diagram of 64 QAM modulation with post-distortion $(K = 6, D = 2)$.

3.2. Constellation Map

In the next study, we plot the constellation diagrams with 100 OFDM symbols with 20 dB SNR and 1 dB power back-off. Fig. 6(a) shows the constellation diagram of 64 QAM modulation without post-distortion, (b) shows the constellation diagram of 64 QAM modulation with post-distortion $(K = 6, D = 2)$.

As indicated in Fig. 6(a), the constellation diagram without post-distortion is fuzzy. The BER performance can be significantly degraded as there exists interference among different constellation points. In Fig. 6(b), the constellation diagram with post-distortion is more clear than that without post-distortion.

4. Conclusion

The LED was the major source of nonlinearity in a VLC system. Commercial LEDs exhibited nonlinearity with memory effects as the carrier-density response was frequency depended. In order to track and compensate for the nonlinearity with memory effects, we proposed an adaptive post-distortion technique with memory polynomial model in VLC systems. Compared to the predistortion technique, the post-distortion was cost-efficient as it only needed some additional

computational resources while the predistortion needed some additional physical circuits. The performance of the post-distortion technique was tested in a DCO-OFDM system with 64 QAM modulation and AWGN channel. Simulation results validated that the post-distortion technique significantly improved the EVM and BER performance of the receiver.

References

[1] T. Komine and M. Nakagawa, "Fundamental analysis for visible-light communication system using LED lights," *IEEE Trans. Consum. Electron.*, vol. 50, no. 1, pp. 100–107, Feb. 2004.

[2] F. M. Wu *et al.*, "Performance comparison of OFDM signal and CAP signal over high capacity RGB-LED-Based WDM visible light communication," *IEEE Photonics J.*, vol. 5, no. 4, pp. 7901507, Aug. 2013.

[3] H. Elgala, R. Mesleh, and H. Haas, "Indoor broadcasting via white LEDs and OFDM," *IEEE Trans. Consum. Electron.*, vol. 55, no. 3, pp. 1127–1134, Aug. 2009.

[4] K. Asatani and T. Kimura, "Analyses of LED nonlinear distortions," *IEEE J. Solid-State Circuits*, vol. 13, no. 1, pp. 125–133, Feb. 1978.

[5] N. Theofanous and A. Arapoyianni, "Light-to-input nonlinearities in an R-LED series network," *IEEE J. Quantum Electron.*, vol. 28, no. 1, pp. 34–38, Jan. 1992.

[6] Z. Ghassemlooy, W. O. Popoola, and S. Rajbhandari, *Optical Wireless Communications-System and Channel Modelling With MATLAB*. Boca Raton, FL, USA: CRC, Aug. 2012.

[7] P. Haigh, Z. Ghassemlooy, S. Rajbhandari, and I. Papakonstantinou, "Visible light communications using organic light emitting diodes," *IEEE Commun. Mag.*, vol. 51, no. 8, pp. 148–154, Aug. 2013.

[8] P. Haigh, Z. Ghassemlooy, and I. Papakonstantinou, "1.4-Mb/s white organic LED transmission system using discrete multitone modulation," *IEEE Photon. Technol. Lett.*, vol. 25, no. 6, pp. 615–618, Mar. 2013.

[9] B. Inan *et al.*, "Impact of LED nonlinearity on discrete multitone modulation," *J. Opt. Commun. Netw.*, vol. 1, no. 5, pp. 439–451, Oct. 2009.

[10] H. Elgala, R. Mesleh, and H. Haas, "A study of LED nonlinearity effects on optical wireless transmission using OFDM," in *Proc. IFIP Int. Conf. Wireless Opt. Commun. Netw.*, Cairo, Egypt, Apr. 2009, pp. 1–5.

[11] T. Kamalakis, J. W. Walewski, G. Ntogari, and G. Mileounis, "Empirical Volterra-series modeling of commercial light-emitting diodes," *J. Lightw. Technol.*, vol. 29, no. 14, pp. 2146–2155, Jul. 2011.

[12] K. Asatani and T. Kimura, "Linearization of LED nonlinearity by predistortions," *IEEE J. Solid-State Circuits*, vol. 13, no. 1, pp. 133–138, Feb. 1978.

[13] H. Elgala, R. Mesleh, and H. Haas, "Non-linearity effects and predistortion in optical OFDM wireless transmission using LEDs," *Int. J. Ultra Wideband Commun. Syst.*, vol. 1, pp. 143–150, Oct. 2009.

[14] G. Stepniak, J. Siuzdak, and P. Zwierko, "Compensation of a VLC phosphorescent white LED nonlinearity by means of Volterra DFE," *IEEE Photon. Technol. Lett.*, vol. 25, no. 16, pp. 1597–1600, Aug. 2013.

[15] R. Mesleh, H. Elgala, and H. Haas, "On the performance of different OFDM based optical wireless communication systems," *IEEE/OSA J. Opt. Commun. Netw.*, vol. 3, no. 8, pp. 620–628, Sep. 2011.

[16] M. Schetzen, "Nonlinear system modeling based on the Wiener theory," *Proc. IEEE*, vol. 69, no. 12, pp. 1557–1573, Dec. 1981.

[17] E. Costa and S. Pupolin, "M-QAM-OFDM system performance in the presence of a nonlinear amplifier and phase noise," *IEEE Trans. Commun.*, vol. 50, no. 3, pp. 462–472, Mar. 2002.

[18] H. Elgala, R. Mesleh, and H. Haas, "An LED model for intensity-modulated optical communication systems," *IEEE Photon. Technol. Lett.*, vol. 22, no. 11, pp. 835–837, Jun. 2010.

[19] L. Ding, R. Raich, and G. T. Zhou, "A Hammerstein predistortion linearization design based on the indirect learning architecture," in *Proc. IEEE ICASSP*, vol. 3, May 2002, pp. III-2689–III-2692.

[20] L. Ding *et al.*, "A robust digital baseband predistorter constructed using memory polynomials," *IEEE Trans. Commun.*, vol. 52, no. 1, pp. 159–165, Jan. 2004.

[21] V. J. Mathews, "Adaptive polynomial filters," *IEEE Signal Process. Mag.*, vol. 8, no. 3, pp. 10–26, Jul. 1991.